2008 IEEE International Conference on
Robotics and Automation
Pasadena, CA, USA, May 19-23, 2008

Safe Joint Mechanism based on Nonlinear Stiffness for Safe Human-Robot Collision

Jung-Jun Park, Yong-Ju Lee, Jae-Bok Song, and Hong-Seok Kim

Abstract—**In recent years, collision safety has been one of the most important issues for service robots. To ensure collision safety assurance, a passive compliance method is preferred to an active one because it can provide faster and more reliable responses to dynamic collision. Since both positioning accuracy and collision safety are equally important, a robot arm should have very low stiffness when subjected to a collision force greater than the one causing human injury, but maintain very high stiffness otherwise. In order to realize these ideal features, a novel safe joint mechanism (SJM) composed of linear springs and a modified slider-crank mechanism is proposed in this paper. The SJM has the advantages of variable stiffness which can be achieved only by passive mechanical elements. Various experiments on static and dynamic collisions show the high stiffness of the SJM against an external force of less than the critical impact force, but an abrupt drop in the stiffness when the external force exceeds this critical force, which guarantees positioning accuracy and collision safety. Furthermore, the critical impact force can be set to any value depending on the application and the environment.**

I. Introduction

In service robotics, safe human-robot coexistence has become one of the most important issues because service robots often interact directly with humans for various tasks. Therefore, several types of compliant joints and flexible links of a manipulator have been proposed for collision safety.

A safe robot arm can be achieved by either a passive or active compliance system. In the actively compliant arm, collision is detected by various types of sensors, and the stiffness of the arm is properly controlled. The active compliance-based approach suffers from slow response, noise problems, actuator malfunction and high cost. To cope with these drawbacks, a collision detection method that used only proprioceptive sensors and provided the information on the direction of the robot reaction after collision was proposed [1]. However, some problems of active compliance approaches still remain unsolved.

This research was supported by the Personal Robot Development Project funded by the Ministry of Commerce, Industry and Energy of Korea.

Jung-Jun Park is with the Dept. of Mechanical Eng., Korea University, Seoul, Korea (e-mail: hantiboy@korea.ac.kr)

Yong-Ju Lee is with the Dept. of Mechanical Eng., Korea University, Seoul, Korea (e-mail: yongju_lee@korea.ac.kr)

Jae-Bok Song is a Professor of the Dept. of Mechanical Eng., Korea University, Seoul, Korea (Tel.: +82 2 3290 3363; fax: +82 2 3290 3757; e-mail: jbsong@korea.ac.kr)

Hong-Seok Kim is a Division Head of Control and Intelligence Research Team, Korea Institute of Industrial Technology, Ansan, Korea. (e-mail: hskim@kitech.re.kr)

On the other hand, the safety device based on passive compliance usually consists of the mechanical components such as a spring and a flexible material, which can attenuate the unexpected collision force. Several attempts for passive compliance have been suggested so far. The mechanical impedance adjuster with a variable spring and an electromagnetic brake was developed [2]. The programmable, passive compliance-based shoulder mechanism using an elastic link was proposed [3]. A passive compliance joint with rotary springs and a MR damper was suggested for the safe arm of a service robot [4]. A variable stiffness actuator with the nonlinear torque transmitting system composed of a spring and a belt was developed [5]. The compliance method in the drive system so as to mechanically decouple the heavy actuator inertia from the link inertia was also introduced [6].

Linear springs have been used for most passive compliance based devices. To absorb a collision force, a low stiffness spring should be used. However, a serious drawback to the use of this type of a linear spring is positioning inaccuracy due to the continual operation of a spring even for small external forces that do not require any shock absorption and due to undesirable oscillations caused by the elastic behavior of a spring. To cope with this problem, some systems adopted extra sensors and actuators such as electric motors, dampers or brakes, which significantly impair the advantages of a passive system.

An ideal safe manipulator would exhibit very low stiffness when subjected to a collision force greater than the one that may cause injury to humans, but maintain very high stiffness otherwise. Of course, this ideal feature can be achieved by the active compliance approach, but this approach often causes the several shortcomings mentioned above. In the previous research, this ideal feature was realized by a novel design of the safe link mechanism (SLM) which was based on the passive compliance [7]. However, a safe mechanism, which is simpler and more lightweight than SLM, is required for a service robot arm.

In this research, a novel safety mechanism, safe joint mechanism (SJM), is proposed. The SJM possesses the same characteristics as SLM to implement the above requirements. The SJM is composed of the passive mechanical elements such as linear springs and a modified slider-crank mechanism. The springs are used to absorb the large collision force for safety, while the slider-crank mechanism determines whether the safety feature is activated or not so that the SJM operates only in case of an emergency. The main contribution of this

978-1-4244-1647-9/08/$25.00 ©2008 IEEE.

proposed device is the variable stiffness capability implemented only by use of simple passive mechanical elements. Without sacrificing positioning accuracy for safety, both features can be achieved simultaneously with the SJM.

The rest of this paper is organized as follows. The operational principle of the SJM is discussed in detail in section II. Section III presents further explanation about its prototype modeling and compliance analysis. Various experimental results for both static and dynamic collisions are provided in section IV. Finally, section V presents conclusions and future work.

II. Operational Principle of Safe Joint Mechanism

The passive compliance mechanism proposed in this research consists of a spring and a modified slider-crank mechanism. This chapter presents the concept of the transmission angle of a slider-crank mechanism and the characteristics of the modified slider-crank mechanism in combination with a spring.

Springs have been widely used to absorb shock of various mechanical systems. Since the displacement of a linear spring is proportional to an external force, the robot arm exhibits deflection due to its own weight and/or payload when a spring is installed at the manipulator joint. This characteristic is beneficial to a safe robot arm, but has an adverse effect on positioning accuracy. To cope with this problem, it is desirable to develop a nonlinear spring whose stiffness remains very high when the external force acting on the end-effector is within the range of normal operation, but becomes very low when it exceeds a certain level of force due to collision with the object. However, no such springs with this ideal feature exist. In this research, the power transmission characteristics of a 4-bar linkage are exploited to achieve this nonlinear spring feature.

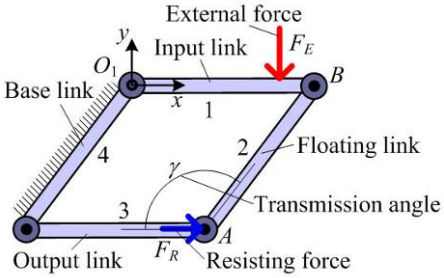

Fig. 1 4-bar linkage.

Consider a 4-bar linkage mechanism shown in Fig. 1. When an external force F_E is exerted on the input link in the y-axis direction, an appropriate resisting force F_R acting on point A of the floating link in the x-axis direction can prevent the movement of the output link. In the 4-bar linkage, the transmission angle is defined as the angle between the floating and the output link. The power transmission efficiency from input to output varies depending on this transmission angle [7].

The slider-crank linkage can be regarded as the 4-bar linkage if the slider is replaced by an infinitely long link perpendicular to the sliding path as shown Fig. 2. Note that the transmission angle of a slider-crank mechanism can be also defined as the angle between the floating link (link 2) and the output link (link 3). The balance between forces acting on the slider and the input link can be given by

$$F_R = -\frac{d}{l_1} F_E \tan\gamma \tag{1}$$

where d is the distance between point O_1 and P on which the external force F_E acts and l_1 is the length of link 1. In Eq. (1), for the same external force, the resisting force changes as a function of γ and d.

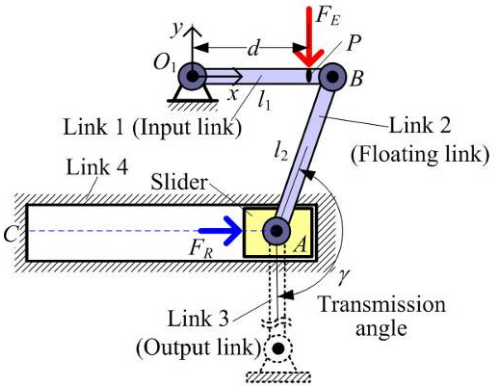

Fig. 2 Slider-crank mechanism.

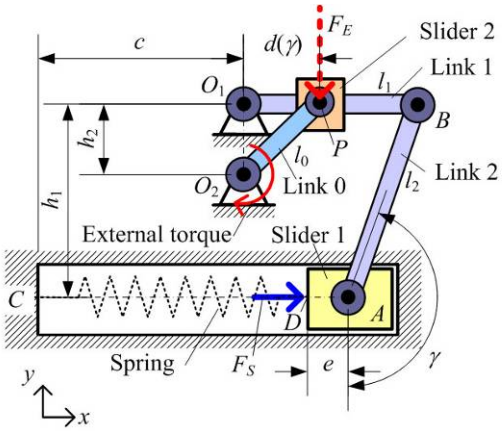

Fig. 3 Slider-crank mechanism combined with spring.

To provide the external force in the vertical direction of link 1, another slider-link which can transmit an external torque is attached to link 1 in Fig. 3. If the pre-compressed spring is installed between points C and D, the spring force F_S can offer the resisting force F_R, which resists the movement of the slider caused by the external force F_E. When the external force is balanced against the spring force, the external force can be described in terms of the transmission angle and the other geometric parameters as follows:

$$F_E = \frac{kl_1}{d(\gamma)}\left(c - e - s_o + \sqrt{l_1^2 + (h_1 + l_2\cos\gamma)^2} - l_2\sin\gamma\right)\cot\gamma \qquad (2)$$

where k is the spring constant, s_o the initial length of the spring and l_2 the length of link 2. The distance $d(\gamma)$ between points O_1 and P is directly related to γ by the following equation, which can be obtained from the geometric configurations of the modified slider-crank mechanism.

$$d(\gamma) = \frac{h_2(h_1 + l_2\cos\gamma)}{l_1} + \sqrt{\frac{h_2^2(h_1 + l_2\cos\gamma)^2}{l_1^2} - h_2^2 + l_0^2} \qquad (3)$$

where l_0 is the length of link 0. For example, when k = 100N/m, l_1 = 25mm, l_2 = 20mm, l_0 = 15mm, s_0 = 80mm, c = 20mm, e = 6mm h_1= 20mm and h_2 = 10mm, the external force for static force balance can be plotted as a function of γ in Fig. 4. The spring force does not need to be specified for static balance because it is automatically determined for a given γ. As shown in the figure, the external force diverges rapidly to positive infinity as γ approaches 180°, so even a very small spring force can make this mechanism statically balanced against a very large external force. In this research, the transmission angle in the range of 160° to 170° is mainly used in consideration of the mechanical strength of the mechanism.

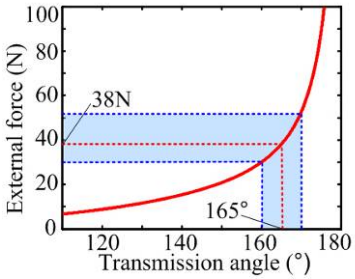

Fig. 4 External force as a function of transmission angle.

In this proposed mechanism, the external force required to balance with the spring force is defined as the *critical impact force*. For a given γ, a static balance is maintained when the external force equals the critical impact force, as shown in Fig. 4, but the spring is rapidly compressed once the external force greater than this critical value acts on this mechanism. The detailed explanation about the motion of this slider-crank mechanism combined with a spring is given below.

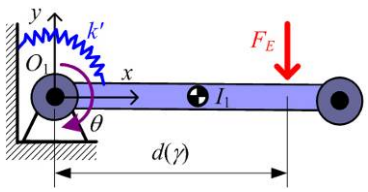

Fig. 5 Simplified model of slider-crank mechanism combined with spring.

Since link 1 is a large portion of the proposed SJM, its mass is much larger than those of sliders and other links in Fig. 3. It is, therefore, assumed that only the mass of link 1 is considered. In this case, the motion of the slider-crank mechanism combined with a spring can be simply modeled as a 1 DOF mass-spring system, as shown in Fig. 5. The resisting spring force acting on slider 1 in Fig. 3 is transmitted to link 1 via link 2 whose transmission angle affects the force transmission ratio. Therefore, the equivalent stiffness of this model can be given by

$$k' = -\frac{d\tau}{d\theta} = -\frac{d(F_E \cdot d(\gamma))}{d\theta} \qquad (3)$$

Since the angular displacement θ of link 1 and the transmission angle γ of the slider-crank mechanism are related by $\gamma = \cos^{-1}((l_1\sin\theta - h_1)/l_2)$, the equivalent stiffness k' of the spring attached to link 1 can be described by

$$k' = -kl_1\left[\left(\frac{l_1(h_1 + l_2\cos\gamma)\cos\theta}{\sqrt{l_1^2 + (h_1 + l_2\cos\gamma)^2}} + l_1\cos\theta\cot\gamma\right)\cot\gamma + \left(c - e - s_0 + \sqrt{l_1^2 + (h_1 + l_2\cos\gamma)^2} - l_2\sin\gamma\right)\frac{l_1\cos\theta}{l_2\sin^3\gamma}\right] \qquad (4)$$

where l_1, l_2, h_1, h_2, c, e, s_0 and k are the same parameters as in Eq. (2) and (3).

Figure 6(a) shows the equivalent stiffness curves as a function of angular displacement of link 1. In this analysis, each parameter is set to the same value as the above example. The equivalent stiffness is maintained very high for a small angular displacement of link 1, but it quickly drops as the angular displacement increases. Hence this nonlinear stiffness can be realized by the slider-crank mechanism combined with a spring.

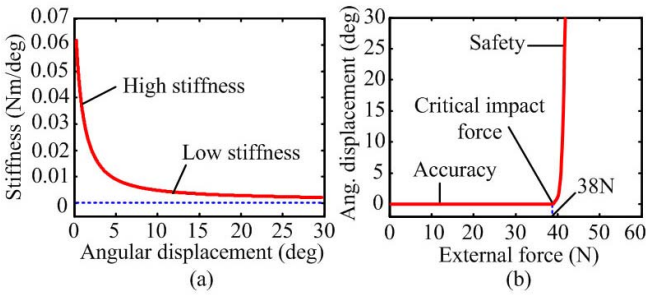

Fig. 6 Analysis of slider-crank mechanism combined with spring; (a) equivalent stiffness of SJM as a function of angular displacement, and (b) angular displacement versus external force.

As the external force acting on link 1 increases linearly up to 60N during 1sec, the displacement is changed as shown in Fig. 6(b). Since the critical impact force was set to 38N in this

simulation, the transmission angle for the static equilibrium becomes 165° from Eq. (2). When the external force increases from 0 to 38N, which is below the critical impact force, link 1 does not rotate. As the external force $F_E(t)$ increases above the critical impact force, the static equilibrium cannot be maintained and the link 1 starts rotating. Since the stiffness of the spring rapidly decreases, as shown in Fig. 6(a), link 1 rotates clockwise rapidly. In summary, the SJM stiffness remains very high like a rigid joint while the external force is below 38N, but as the external force becomes larger than 38N, the stiffness abruptly diminishes, thus causing the SJM to behave as a flexible joint.

III. Model of Safe Joint Mechanism

A. Prototype modeling

The mechanisms introduced conceptually in the previous section are now integrated into the safe joint mechanism (SJM), which suggests a new concept of a safe robot arm. The SJM consists of a slider-crank mechanism and a linear spring. As shown in Fig. 7, the slider-crank mechanism is installed at the fixed plate which is joined with a non-backdrivable joint actuator and the robot link is connected to the rotating plate. The collision force can be transmitted to the slider-crank mechanism by means of the force transmission shaft fixed at the rotating plate. The slider-crank mechanisms are arranged symmetrically so that they can absorb the collision force applied in both directions.

In this prototype, the collision force acting on the end-effector is amplified according to the ratio of the rotation radius of the force transmission shaft to that of the end-effector, and is transmitted to link 1 by the force transmission shaft. Therefore, the external force exerted on the SJM is proportional to the collision force.

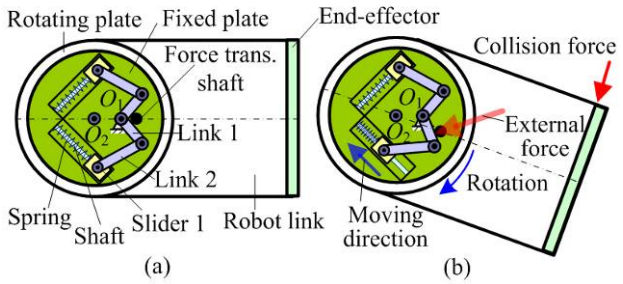

Fig. 7 Operation of SJM; (a) before collision, and (b) after collision.

If the external force exceeding the critical impact force is applied to link 1 of the slider-crank mechanism by the force transmission shaft connected to the rotating plate, then link 1 is rotated around point O_1, as shown in Fig. 7(b). Then, slider 1 connected to link 2 is forced to move left on the guide shaft to compress the spring. This movement of slider 1 reduces the transmission angle, so maintaining the static balance requires a greater resisting force for the same external force. However, the increased spring force due to its compression is not large enough to sustain the balance. This unbalanced state causes the slider to rapidly slide left. As a result, the force transmission shaft fixed at the rotating plate is rotated and the robot link is also rotated, which absorbs the collision force. However, if the external force amplified from the collision force is less than the critical impact force, the end-effector does not rotate at all, and the slider-crank mechanisms maintain the static equilibrium, so the SJM can provide high stiffness for the joint of the robot arm.

B. Compliance analysis

The 2-DOF robot arm with the SJM is modeled in Fig. 8 to analyze the change in its compliance. The motors transmit the torque to each joint, and the SJM is attached to only motor 2 at joint 2.

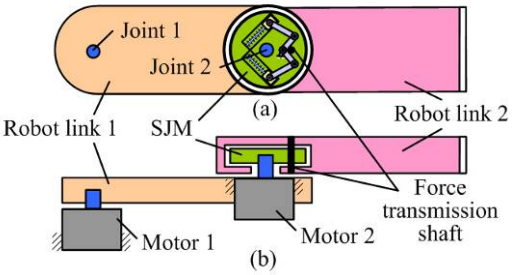

Fig. 8 2-DOF robot arm with SJM; (a) top view and (b) side view.

The stiffness k_1 and k_2 of joint 1 and 2, respectively, can be adjusted by control of each motor. If a collision force larger than the critical impact force is applied to the end-effector, then the SJM operates and robot link 2 rotates as shown in Fig. 7(b). In this case, the stiffness of joint 2 is replaced by that of the SJM which can be computed by Eq. (4). Since the stiffness of each joint is independent of each other, the joint stiffness matrix is given by

$$\mathbf{K_q} = \begin{bmatrix} k_1 & 0 \\ 0 & k_2 \end{bmatrix} \tag{5}$$

The compliance matrix (i.e., inverse of Cartesian stiffness matrix) in the Cartesian coordinate frame can be defined as

$$\mathbf{K}^{-1} = \mathbf{J}\mathbf{K}_\mathbf{q}^{-1}\mathbf{J}^\mathbf{T} \tag{6}$$

where **J** is the Jacobian matrix. Solving the eigenvalue problem, the compliance ellipsoid can be drawn from the eigenvalues and eigenvectors. The compliance ellipsoid (compliance ellipse in this 2 DOF system) is useful for the safety analysis of a robot arm. The length of the major axis of the ellipsoid represents the maximum compliance, while the length of the minor axis determines the minimum compliance. Therefore, the longer the length of the major axis, the more

safety is provided to the system.

Figure 9 shows some compliance ellipsoids according to the angular displacement of the SJM when the angle of joint 1 is fixed at 45° and the collision force acts on the end-effector. In this analysis, the spring constant k is set to 10kN/m, the length of robot link 1 to 300mm, that of robot link 2 to 300mm, the initial transmission angle to 165°, and the stiffness of each motor to 52.4Nm/deg (=3kNm/rad).

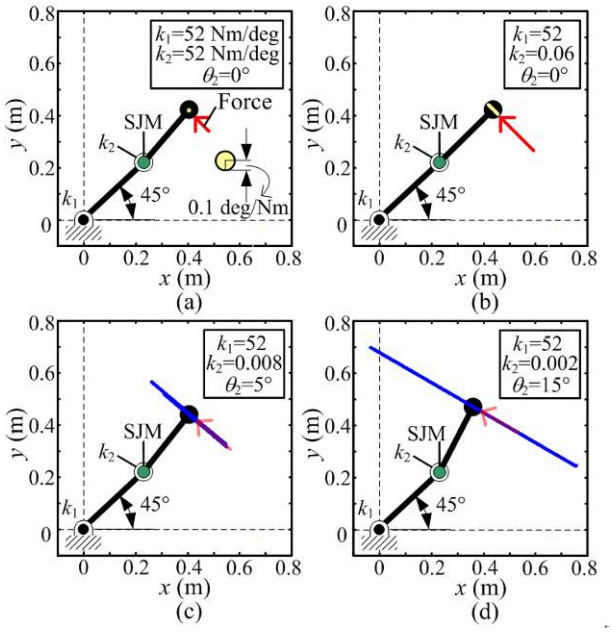

Fig. 9 Compliance ellipsoid of a manipulator equipped with SJM.

When the external force amplified from the collision force is less than the critical impact force, the stiffness of joint 2 is the same as that of the joint actuator because of the characteristics of the SJM. For this reason, the length of the major axis of the ellipsoid becomes very short, and consequently, high positioning accuracy of the robot arm can be achieved in normal operation, as shown in Fig. 9(a).

However, when the external force exceeds the critical impact force, the angular displacement of the SJM occurs and its stiffness rapidly drops owing to the operation of the SJM. As shown in Fig. 9(b) ~ (d), as the angular displacement increases, the length of the major axis of the compliance ellipsoid increases rapidly. Therefore, collision safety can be improved by the use of SJM.

IV. Experiments for Safe Joint Mechanism

A. Prototype of SJM

The prototype of the SJM shown in Fig. 10 was constructed to conduct various experiments related to the performance of the SJM. Most components are made of duralumin and polyoxymethylene which can endure the shock exerted on the SJM. The slider can slide and the spring can be compressed by means of the linear bushing guides.

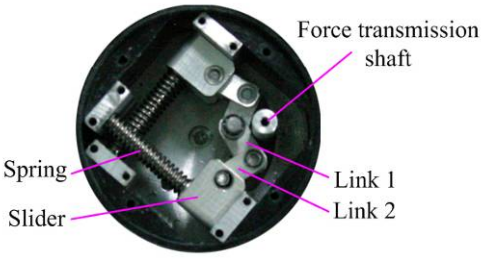

Fig. 10 Prototype of SJM.

B. Safety criterion

The safety criterion can be divided into static and dynamic collisions. In the case of static collision (i.e., the collision speed below 0.6m/s), the human pain tolerance for static collision can be suggested as 50N by several experimental researches [8]. In the case of dynamic collision (above 0.6m/s), the head injury criterion (HIC), which is used to quantitatively measure head injury risk in car crash situations, is adopted in this research [9]. An HIC value of 1,000 or greater is typically associated with extremely severe head injury, and a value of 100 can be considered suitable to normal operation of a machine physically interacting with humans.

C. Experimental results

To conduct experiments on collision safety, the SJM is installed at the 1-DOF robot arm in the manner discussed in section III-A. Therefore, the torque of a motor can be transmitted to the robot link via the SJM. A force/torque sensor installed at the bottom of the wall measures the collision force, as shown in Fig 11. The angular displacement of the SJM is measured by an encoder attached to the SJM.

In the experiment for static collision, the spring constant was 10kN and the initial transmission angle was set to 165°. The end-effector of the robot link was initially placed to barely touch a fixed wall, and its joint torque provided by the motor was slowly increased. The static collision force between the robot link and the wall was measured by the 6 axis force/torque sensor. Experiments were conducted for the robotic arms with and without the SJM.

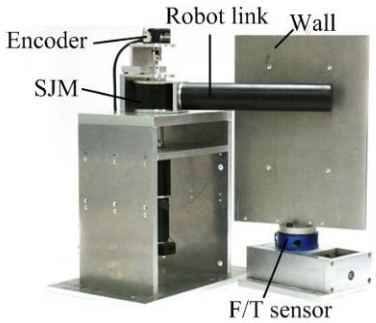

Fig. 11 Experimental setup for robot arm with SJM.

Without the SJM, the contact force increased beyond the human pain tolerance, as shown in Fig. 12(a). However, the

contact force of only up to 32N was transmitted to the wall for the robot arm with the SJM, as shown in Fig. 12(a). In other words, the contact force is maintained below the pain tolerance because the excessive force is attenuated by the SJM. In Fig. 12(b), virtually no angular displacement of the SJM occurs when the contact force is below the critical impact force. Therefore, the position of the robot arm with the SJM can be accurately controlled while handling a payload up to about 2kg like a very rigid joint. However, as the contact force rises above the critical impact force, the SJM stiffness quickly diminishes and the angular displacement occurs, thus ensuring human safety. In summary, the SJM provides high positioning accuracy of the robot arm in the working region, and guarantees safe human-robot contact by absorbing the contact force above 50N in the unsafe region.

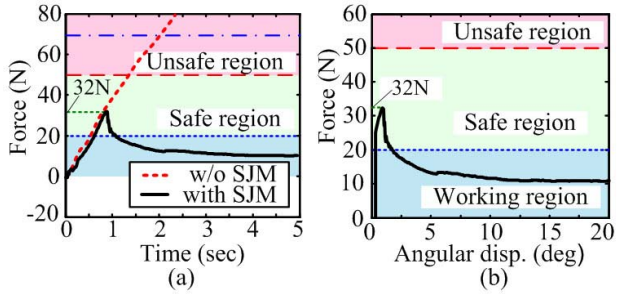

Fig. 12 Experimental results for static collision for robot arm; (a) collision force versus time without and with SJM, and (b) collision force versus angular displacement of SJM.

Next, some experiments on dynamic collision were conducted for the robot arm equipped with the SJM. For dynamic collision, a urethane ball of 2.5kg moving at a velocity of 3m/s was forced to collide with the end-effector of the robot arm. The acceleration of the ball was measured by the accelerometer mounted at the ball.

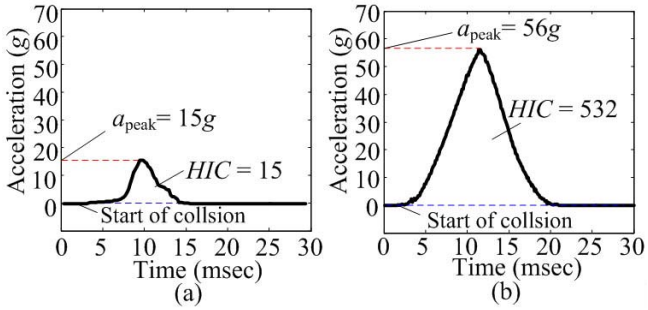

Fig. 13 Experimental results for dynamic collision of robot arm; acceleration versus time (a) with SJM, and (b) without SJM.

Figure 13(a) shows the experimental result for the dynamic collision of the robot arm with the SJM. The HIC value was computed as 15, which is far less than 100. Therefore, the safe human-robot contact can be achieved even for this harsh dynamic collision.

The experimental result for the robot arm without the SJM is shown in Fig. 13(b). The peak value of the acceleration is almost quadruple that of the robot arm with the SJM, and the HIC value reached as high as 532, which indicates a high risk of injury to a human. Therefore, the robot arm with the SJM provides much greater safety for human-robot contact than that without the SJM.

V. Conclusions

In this research, a new safe joint mechanism (SJM) was proposed, which can provide collision safety and positioning accuracy simultaneously. From the analysis and experiments, the following conclusions are drawn:

1) The SJM maintains very high stiffness like a rigid joint up to the pre-determined critical impact force. Therefore, high positioning accuracy of the robot arm can be achieved in normal operation.

2) When the external force exceeds the critical impact force, the stiffness of the SJM abruptly drops. As a result, the robot arm acts as a compliant joint with high compliance. Therefore, human-robot collision safety can be attained even for high-speed dynamic collision.

3) The proposed SJM is based on passive compliance, so it shows faster response and higher reliability than that based on the active compliance having sensors and actuators.

4) Since the SJM is simply installed between the actuator and the robot link, it can be applied to the existing robot arms by small change of the robot design.

Currently, simpler and more lightweight models are under development.

References

[1] A. De Luca, A. Albu-Schaffer, S. Haddadin and G. Hirzinger, "Collision detection and safe reaction with the DLR-III lightweight manipulator arm," *Proc. of the IEEE/RSJ International Conference on Intelligent Robots and System*, pp. 1623-1630, 2006.

[2] T. Morita and S. Sugano, "Development of one-D.O.F. robot arm equipped with mechanical impedance adjuster", *Proc. of the IEEE/RSJ International Conference on Intelligent Robots and System*, pp. 407-412, 1995.

[3] M. Okada, Y. Nakamura and S. Ban, "Design of programmable passive compliance shoulder mechanism", *Proc. of the IEEE International Conference on Robotics and Automation*, pp.348-353, 2001.

[4] S. Kang and M. Kim, "Safe Arm Design for Service Robot", *Proc. of the International Conference on Control, Automation and System*, pp.88-95, 2002.

[5] G. Tonietti, R. Schiavi and A. Bicchi, "Design and Control of a Variable Stiffness Actuator for Safe and Fast Physical Human/Robot Interaction", *Proc. of the IEEE International Conference on Robotics and Automation*, pp. 528-533, 2005.

[6] M. Zinn, O. Khatib, B. Roth and J. K. Salisbury, "A new actuation approach for human-friendly robot design," *International Journal of Robotics Research*, vol. 23, no. 4/5, pp. 379-398, 2005.

[7] J. Park, B. Kim and J. Song, "Safe Link Mechanism based on Passive Compliance for Safe Human-Robot Collision", *Proc. of the IEEE International Conference on Robotics and Automation*, pp. 1152-1157, 2007.

[8] Y. Yamada, Y. Hirasawa, S.Y. Huang and Y. Umetani, "Fail-safe human/robot contact in the safety space", *IEEE International Workshop on Robot and Human Communication*, pp. 59-64, 1996.

[9] J. Versace, "A review of the severity index", *Proc. of the 15th Stapp Car Crash Conference*, pp.771–796, 1971.